tvst

Article

RTVue XR AngioVue Optical Coherence Tomography Angiography Software Upgrade Impacts on Retinal Thickness and Vessel Density Measurements

Danuta M. Sampson[1,2], Noha Ali[1,3], Alex Au Yong[1], Rumaanah Jeewa[1], Saumya Rajgopal[1], Deepaysh D. C. S. Dutt[1], Sharaf Mohamed[3], Shehata Mohamed[3], Alex Hansen[4], Moreno Menghini[1,4], and Fred K. Chen[1,5,6]

[1] Centre for Ophthalmology and Visual Science (incorporating Lions Eye Institute), The University of Western Australia, Nedlands, Western Australia, Australia
[2] Surrey Biophotonics, Centre for Vision, Speech and Signal Processing and School of Biosciences and Medicine, The University of Surrey, Guildford, UK
[3] Department of Ophthalmology, Faculty of Medicine, Assiut University, Assiut, Egypt
[4] Department of Ophthalmology, Sir Charles Gairdner Hospital, Nedlands, Western Australia, Australia
[5] Department of Ophthalmology, Royal Perth Hospital, Perth, Western Australia, Australia
[6] Department of Ophthalmology, Perth Children's Hospital, Perth, Western Australia, Australia

Correspondence: Fred K. Chen, Lions Eye Institute, 2 Verdun St, Nedlands, WA 6009, Australia. e-mail: fredchen@lei.org.au

Received: June 28, 2019
Accepted: November 18, 2019
Published: February 12, 2020

Keywords: OCTA; optical coherence tomography angiography; Optovue, AngioVue; retinal capillary density; split-spectrum amplitude decorrelation angiography; normative data

Citation: Sampson DM, Ali N, Au Yong A, Jeewa R, Rajgopal S, Dutt DDCS, Mohamed S, Mohamed S, Hansen A, Menghini M, Chen FK. RTVue XR AngioVue optical coherence tomography angiography software upgrade impacts on retinal thickness and vessel density measurements. Trans Vis Sci Tech. 2020;9(3):10, https://doi.org/10.1167/tvst.9.3.10

Purpose: To determine the impact of an AngioVue software upgrade on total retinal thickness (RT) and inner retinal vessel density (VD) measurements derived from optical coherence tomography angiography (OCTA).

Methods: Optovue OCTA images (3 × 3 mm) from 126 individuals (105 healthy eyes and 72 eyes with retinal disease) were acquired before an upgrade of the AngioVue software, which resulted in an inward shift of the outer boundary of the inner retinal vessels and improved Bruch's membrane segmentation. Total RT and inner retinal VD values were extracted before and after the software upgrade for comparison. Bias and limits of agreement (LA) were calculated.

Results: The mean (SD) age of participants was 46 (17) years. Mean (LA) foveal RT increased by 3.0 (−11 to +17) and 3.7 (−11 to +18) µm ($P < 0.001$) and parafoveal RT increased by 9.7 (−3.8 to +23) and 6.4 (−2.5 to +15) µm ($P < 0.001$) in healthy and diseased retina, respectively. Mean (LA) foveal inner retinal VD decreased by 6.6 (2.5–11) and 7.7 (0.4–15) percentage units ($P < 0.001$) and parafoveal inner retinal VD decreased by 4.1 (1.2–7.0) and 4.7 (0.5–8.9) percentage units ($P < 0.001$) in healthy and diseased retina, respectively.

Conclusions: The AngioVue software upgrade resulted in an unexpected increase in total RT and an expected reduction in inner retinal VD measurements in all regions due to altered segmentation.

Translational Relevance: RT and VD measures derived from the newer AngioVue software version are not directly comparable to the reported normative data derived from the older software.

Introduction

Retinal diseases often affect thickness of the retina; therefore, mapping and measurement of the retinal layer thickness is important in diagnosis and disease management.[1–4] Similarly, quantitative characterization of the retinal vessel density plays an important role in detecting and monitoring the development of subclinical retinal vascular diseases, including diabetic

retinopathy and branch retinal vain occlusion.[5–8] The easy accessibility to optical coherence tomography (OCT) and OCT angiography (OCTA) systems has transformed clinical practice; however, quantitative analysis is only meaningful if the onboard software can delineate boundaries within the retina accurately and reliably.

The AngioVue™ Imaging System (RTVue XR Avanti, Optovue Inc., Fremont, CA, USA) is a spectral-domain optical coherence tomography (SD-OCT) device that enables simultaneous three-dimensional (3D) structural imaging of the retina and generation of en face maps of blood flow through a split-spectrum amplitude decorrelation angiography algorithm.[9] The AngioVue software allows retinal thickness (RT) and vessel density (VD) to be calculated from selected regions of the retina. Several reports have been published on normative values delivered by the instruments, and many studies have examined the intra- and inter-session repeatability of retinal layer thickness and superficial capillary density measurements from the RTVue XR Avanti SD-OCT.[2,7,8,10–16] Based on recent clinicohistological correlations, Campbell et al.[17] redefined the boundaries among four retinal capillary plexuses. These new boundaries were adopted by the AngioVue software upgrade from Phase 6.5 to Phase 7.0 and applied to VD measurements of the inner retinal vasculature. In the previous software version, the superficial retinal vessel (SRV) slab incorporated flow signals from three separate anatomic layers, including nerve fiber, ganglion cell, and inner plexiform layers. The outer limit of this inner retinal vasculature was shifted inward (toward the inner limiting membrane), from the inner nuclear layer to the inner plexiform layer, and was renamed the superficial vascular complex (SVC) slab, as it includes two vascular plexuses: radial peripapillary capillary plexus and superficial vascular plexus. Consequently, the outer retinal vasculature slab increased in thickness and was renamed the deep vascular complex, comprised of the intermediate capillary plexus and deep capillary plexus. Likewise, segmentation lines for various sublayer RT measurements have been updated (from four to eight), and these changes have had an impact on the appearance of the OCTA and OCT en face slabs. Segmentation of the inner limiting membrane and Bruch's membrane boundaries was unaltered. Another improvement in the AngioVue Phase 7.0 software upgrade is the provision for manual segmentation and a propagation tool to allow efficient correction of segmentation error and enhancement of en face image accuracy.

There is no doubt that this software upgrade may enhance diagnostic sensitivity, as the new segmentation boundaries closely mirror the vascular layers seen in histological sections.[17,18] However, the impact of this segmentation algorithm change on total RT and inner retinal VD measurements remains unknown. Furthermore, the new software recalculates the existing datasets collected before the upgrade but does not save the previous RT and VD calculations derived from the older software version. Therefore, it is important to know the magnitude of the change in RT and VD from altered segmentation so that measurements derived from data collected after software upgrade can be compared to the normative ranges for total RT and inner retinal VD established with the older software. To estimate the change in RT and VD arising from the altered segmentation algorithm in the RTVue XR Avanti SD-OCT device, we compared these measurements obtained from the same OCT volume data, before and after the software upgrade, and calculated the mean differences and their limits of agreement in clinically healthy and diseased retinas.

Methods

Subjects

This was a retrospective cross-sectional study of retinal OCTA images stored in the image database at a single retina practice. The study protocol (RA/4/20/4275) was reviewed by the Office of Research Enterprise and the institutional review board (IRB) of the University of Western Australia, and it was considered exempt from full ethics review by the board as this was a retrospective review of anonymized imaging and clinical data collected as part of routine clinical care. All patients and their legal guardian (if a minor) gave consent at the time of ophthalmic assessment for their anonymized imaging and clinical data to be used for audit and research. OCTA images from a separate cohort of healthy subjects recruited prospectively to establish a normative database under another study protocol (RA/4/1/8570) approved by the same IRB were also used in this study. These subjects also gave consent for retinal imaging and use of their OCTA image for this research. The research was conducted in accordance with the tenets of the Declaration of Helsinki.

Prior to the software upgrade, we kept an image database of patients who underwent Optovue OCTA imaging and subjects who were recruited for establishing a normative database. All subjects in this database were eligible for inclusion, as their old RT and VD measurements were exported prior to upgrade. If RT and VD measurements from two or more OCTA

images were available for one eye, the result from the first OCTA image was chosen for analysis. This study would not have been possible if we did not keep an old record of the previous measurements, as the upgrade was irreversible; all existing OCTA images were re-segmented automatically with the upgrade, and previous RT and VD measurements were overwritten by the new measurements. The medical charts of these eligible patients were reviewed to confirm that they did not have clinically significant lenticular opacities, corneal opacities, or a history of refractive surgery or intraocular inflammation. Diabetic retinopathy grades of R1, R2, and R3S (stable) were assigned as defined by the National Health Service diabetic eye screening program.[19] Healthy cohorts were recruited prospectively from volunteers and patients attending the eye clinic with no history of ocular disease and normal retinal examination and imaging. All healthy subjects within the database were recruited for a previous prospective study, and they had a best-corrected Early Treatment Diabetic Retinopathy Study (*ETDRS*) letter score of 85 or greater. Those with any macular pathology on structural OCT scan were excluded from the prospective healthy control cohort. All retinal patients and healthy subjects underwent retinal OCTA imaging after pupils were dilated using 1% tropicamide with or without 2.5% phenylephrine eye drops.

Optical Coherence Tomography Angiography Imaging Protocol

OCTA images, 3 × 3 mm, used in this study were acquired using the RTVue XR Avanti system, Version 2016.1.0.26 (Optovue). Each scan set contains a horizontal-priority (fast-x) and a vertical-priority (fast-y) raster OCT volume, and these are combined automatically by the AngioVue software via 3D orthogonal registration (motion correction technology, or MCT), thereby removing bulk motion and generating a merged OCTA image for all dimensions with reduced motion artifacts.

Optical Coherence Tomography Angiography Segmentation

Four segmentation lines are provided by the Phase 6.5 software: inner limiting membrane (ILM), inner plexiform layer (IPL), outer plexiform layer (OPL), and Bruch's membrane; however, the Phase 7.0 software segments the retina into eight layers. The boundaries used to define these layers include the ILM, outer limit of the nerve fiber layer (NFL), outer limit of the IPL, outer limit of the inner nuclear layer (INL), outer limit of the OPL, inner/outer segment (IS/OS), apical boundary of retinal pigment epithelium (RPE), and Bruch's membrane. Definitions of the specific retinal layers are summarized in Supplementary Table S1.

Optical Coherence Tomography Angiography: Acquisition, Post-Processing, and Image-Analysis Tools

In both Phase 6.5 and Phase 7.0 versions of the AngioVue software, DualTrac™ Motion Correction is used to correct for motion artifacts. DualTrac is a two-level approach to correcting motion artifacts. The first level provides real-time correction for rapid eye movements, blinking, or eye drifting by using a real-time eye tracking function. The second level occurs during postprocessing of imaging and corrects smaller levels of motion distortion. MCT registers two volumes that are acquired with orthogonal scanning axes, and their postprocessing further improves the motion correction accuracy and resulting image quality.

AngioAnalytics is the onboard software for the AngioVue OCTA device that offers a number of tools to quantify various retinal vasculature parameters. These parameters, available for Phase 6.5 and Phase 7.0 versions of the software, are summarized in Supplementary Table S2. See Supplementary Table S3 for a more detailed explanation of the terminology used in the older and newer software upgrades. RT and inner retinal VD measurements in the whole image and the various regions of interests were extracted from the device before and after the software upgrade. Superficial retinal vessel density (SRVD) refers to the density parameter extracted prior to the upgrade, and superficial vascular complex density (SVCD) refers to the density parameter extracted after the software upgrade.

Statistical Analyses

Each eye was treated independently because the same image from the same retina was segmented twice and the comparison was made in RT and VD derived from these two segmentation algorithms. Statistical analyses were performed separately for eyes with clinical retinal lesions (diseased retina) and eyes without clinical retinal disease (normal retina). Some patients had unilateral retinal conditions; hence, the diseased eye was allocated to the diseased retina group, and the unaffected eye was allocated to normal retinal group.

Using Bland-Altman plots and limits of agreement, we evaluated agreement between RT values derived from the Phase 6.5 and Phase 7.0 software (ILM–RPE distance [µm]) and SRVD (Phase 6.5) versus

SVCD (Phase 7.0) as the number of bright pixels/total number of pixels in each image (% pixels).[20] These analyses were performed for the 18 regions (whole, fovea, parafovea, six parafoveal subregions, and the nine square zones for the vascular density measures) in the central 3 × 3 mm retina (see Supplementary Fig. S1).

To determine whether bias increased with magnitude, absolute difference was plotted against their means. The bias (mean difference), standard deviation of the differences, and 95% confidence limits for the bias (i.e., the limits of agreement, defined as mean difference ± 1.96 SD of the differences) were calculated. The bias and LA are displayed in Figure as solid and dashed lines, respectively. The LA represents the range of values for the differences between the methods that can be expected 95% of the time. The 95% confidence intervals for the mean and the upper and lower LA were also calculated and tabulated. Paired *t*-tests were used to examine the significance of the bias. The *t*-statistic (t_{stat}) is given by

$$t_{stat} = \frac{\bar{d}}{SE\left(\bar{d}\right)} \quad (1)$$

where $\bar{d}$ is the mean difference, and $SE(\bar{d}) = s_d/\sqrt{n}$ is the standard error of the mean difference calculated under the null hypothesis. $P \leq 0.05$ was considered statistically significant.

Relative change as a percentage of initial measurement was also calculated to estimate the impact of the software upgrade:

$$\text{Relative change} = 100 \times \frac{(y - x)}{x} \quad (2)$$

where x and y are the measured retinal thickness and vessel density values before and after the software upgrade, respectively.

Results

Patient Characteristics

Our image database contained 84 OCTA reports on RT and VD from 45 healthy subjects (6 eyes had missing data) and 93 OCTA reports on RT and VD from 50 retinal patients (7 eyes had missing data). A total of 177 OCTA images, including 84 eyes of healthy subjects, 21 eyes with clinically normal retina in patients, and 72 eyes of clinically diseased retina in patients, were included in the analyses (Table 1). Among the 72 eyes with retinal disease, 43 eyes of 24 patients had diabetic retinopathy, 14 eyes of 14 patients had retinal vein occlusion, 7 eyes of 7 patients had adult Coats disease, 4 eyes of 2 patients had retinitis pigmentosa, 2 eyes of a patient had macular dystrophy, 1 eye of a patient had macular telangiectasia, and 1 eye of a patient had radiation retinopathy. The 21 eyes with clinically normal retina came from 13 patients with unilateral retinal vein occlusion, the 7 patients with unilateral adult Coats disease, and the patient with unilateral radiation retinopathy. The mean age (SD, range) of all participants was 46 (17, 10–84) years. The mean (SD, range) visual acuity in ETDRS letter score was 75.1 (11.4, 38–94) letters in the cohort with retinal disease.

Increased Retinal Thickness Measurement

The mean (SD) increase in foveal region RT were 3.00 (7.00) µm in healthy retinas and 3.65 (7.33) µm in diseased retinas ($P < 0.001$ and $P < 0.001$, respectively). The lower and upper bounds of the LA for both groups were –10.72 and +16.72 µm and –10.71 and +18.02 µm, respectively. The mean (SD) increase in parafoveal region RT were 9.74 (6.89) µm in healthy retinas and 6.40 (4.56) µm in diseased retinas, which were also statistically significant for both healthy ($P < 0.05$) and diseased ($P < 0.001$) retinas. The lower and upper bounds of the LA were –3.76 and +23.25 µm and –2.54 and +15.35 µm for healthy and diseased retinas, respectively (Table 2, Fig. 1). There were no obvious relationships between the changes in RT from the software upgrade and image quality based on the new scan quality index (Supplementary Fig. S2).

Relative change (as a percentage of the original values from the old software) in foveal RT ranged from –15.41% to +8.00% for healthy retinas and from –9.25% to +8.31% for diseased retinas (Fig. 2). In the parafoveal region, the relative change varied from –6.98% to +9.17% for healthy retinas and –1.79% to +6.06% for diseased retinas (Fig. 2). Supplementary Table S5 summarizes the measured values for total RT before and after the software upgrade stratified by disease status for each zone.

Reduced Vessel Density Measurement

Foveal SRCD (new software) was lower than foveal SRVD (old software) by mean (SD) differences of –6.60 (2.12) and –7.65 (3.68) % in healthy and diseased retinas, respectively ($P < 0.001$) (Table 3, Fig. 1). The lower and upper bounds of the LA for each group were –10.74 to –2.45% for healthy retinas and –14.85 to –0.44% for diseased retinas. Similarly, parafoveal SVCD was lower than parafoveal SRVD by mean (SD) differences of –4.11 (1.47) % for healthy retinas and

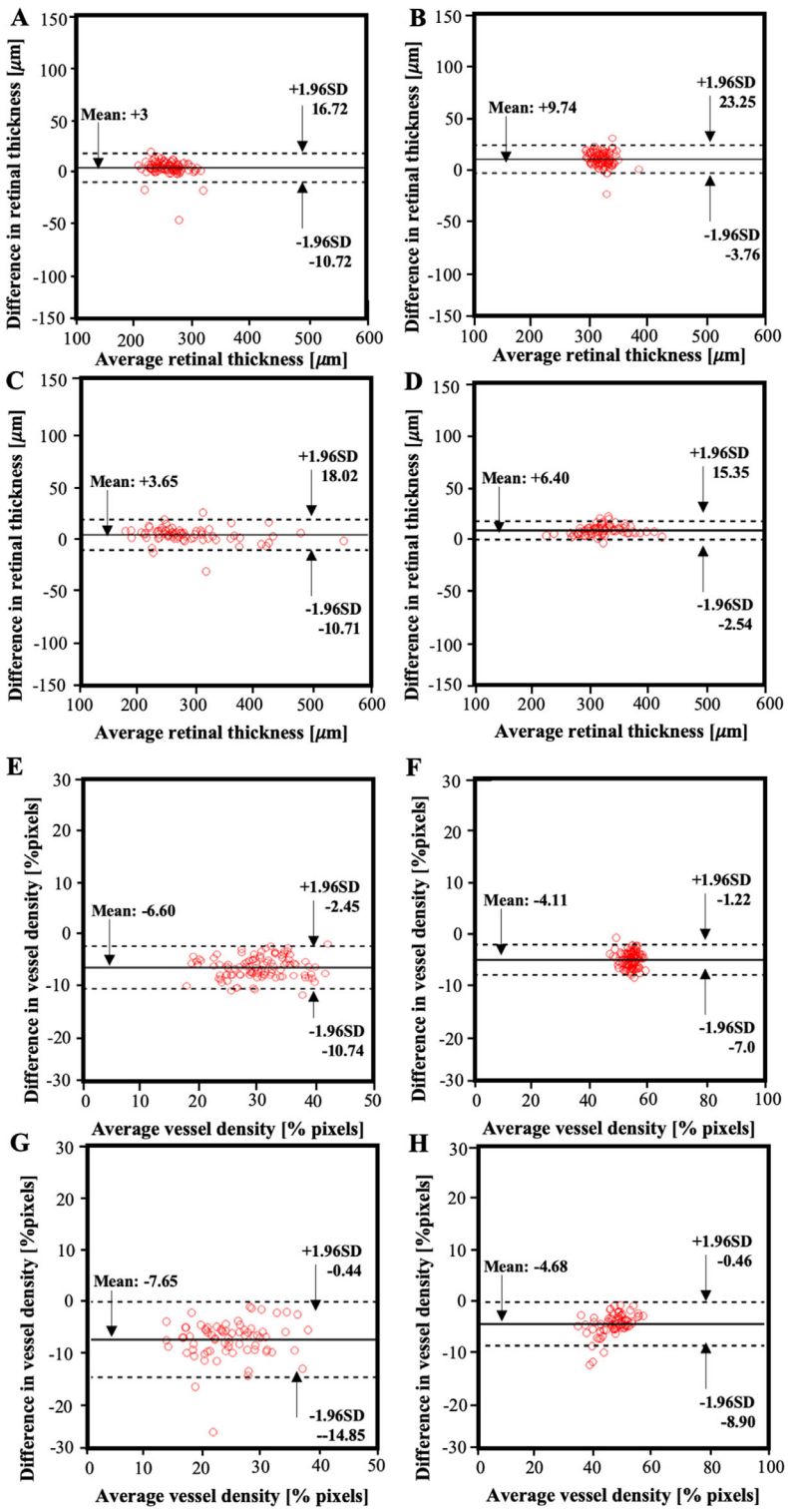

Figure 1. A series of Bland–Altman plots illustrate the agreement in total RT and inner retinal VD before and after the software upgrade. The newer software measures a significantly greater foveal (A) and parafoveal (B) RT in healthy retina. This pattern is also observed in foveal (C) and parafoveal (D) RT in diseased retina. Foveal (E) and parafoveal (F) inner retinal VD are consistently lower when derived from the newer software in healthy retina. The difference remains significant in foveal and parafoveal inner retinal VD in diseased retina (G, H). The solid line is the mean difference (value after upgrade – value before upgrade), and the dotted lines denote 1.96 × standard deviations above and below the mean difference.

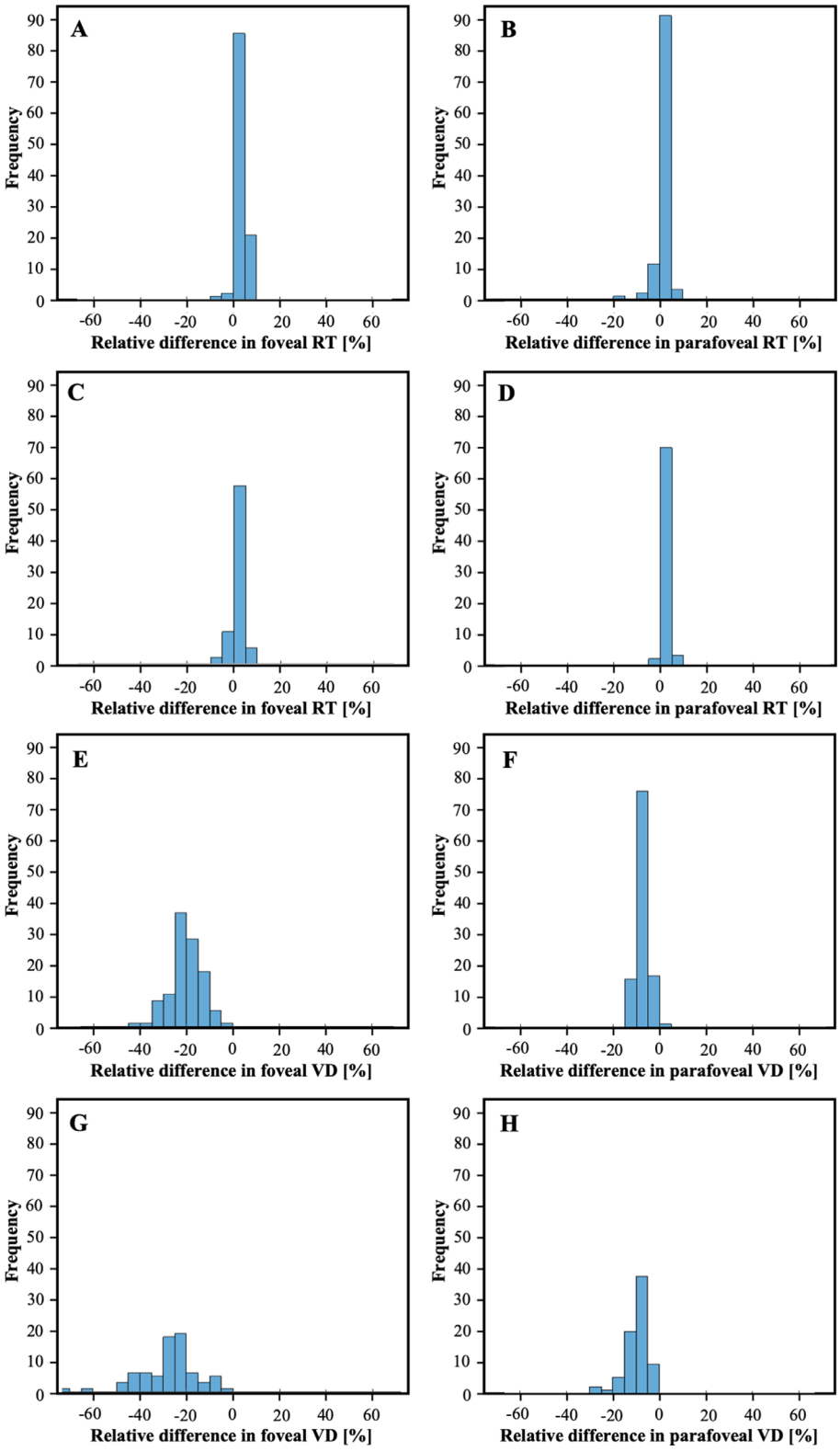

Figure 2. A series of histograms show the frequency of relative percentage change in foveal and parafoveal RT in healthy retina (A, B) and diseased retina (C, D) subjects. Foveal and parafoveal VD in healthy retina (E, F) and diseased retina (G, H) are both significantly lower in the newer software. Relative change is defined by the difference between the values (after – before) divided by the value obtained prior to upgrade.

Table 1. Demographics of Study Subjects

Demographic	Bilateral or Unilateral Healthy Retina	Bilateral or Unilateral Diseased Retina
Number of patients (*n*)	66	50
Age (y), mean (SD)	41.4 (16.6)	56.5 (15.1)
Gender M:F (*n*)	33:33	30:20
Age distribution (*n*)		
<30	23	1
31–40	15	8
41–50	7	7
51–60	10	11
61–70	9	16
>70	2	7
Eyes included in the study (*n*)	105	72
Visual acuity in ETDRS letters, mean (SD)	>85[a]	75.1 (11.4)
Diagnosis (*n*)		
Diabetic retinopathy	NA	43
Retinal vein occlusion	NA	14
Coats disease	NA	7
Others[b]	NA	8
Scan quality (*n*)		
1–4	4	8
5	7	3
6	6	11
7	26	24
8	43	20
9	19	6

NA; not applicable.
[a]Testing of visual acuity in this cohort did not continue beyond 85 letters.
[b]Includes retinitis pigmentosa, macular dystrophy, macular telangiectasia, and radiation retinopathy.

–4.68 (2.15) % for diseased retinas ($P < 0.001$), with lower and upper bounds of the LA of –7.0 to –1.22% for healthy retinas and –8.90 to –0.46% for diseased retinas (Table 3, Fig. 1). A similar mean difference between SRVD and SVCD was observed for each of the nine 1 × 1-mm zones (Supplementary Table S4). There were no obvious relationships between the changes in VD from the software upgrade and image quality based on the new scan quality index (Supplementary Fig. S2).

The relative change (as a percentage of the measurements from the old software) in foveal inner retinal VD ranged from –4.57% to –44.42% in healthy retinas and from –73.85% to +4.86% in diseased retinas. Similarly, the relative change in parafoveal inner retinal VD ranged from –12.83% to +0.45% for healthy retinas and –1.99% to –27.53% for diseased retinas. Figure 3 illustrates the position of the segmentation line marking the outer boundary of the SRV (within INL) and SVC (within IPL) and the density maps generated before and after the upgrade to Phase 7.0 software for two healthy subjects, and Figure 4 shows the same for two selected patients with retinal diseases (see Supplementary Fig. S3 for higher magnification of Figs. 3 and 4). Supplementary Table S6 summarizes the measured values for inner retinal VD before and after the software upgrade stratified by disease status for each zone.

Discussion

The altered segmentation boundary from the software upgrade has had a significant impact on total retinal thickness and inner retinal vessel density measurements. There was an overall significant increase in foveal and parafoveal RT measurements derived from the new software. Furthermore, SVCD generated from the new software was lower than SRVD derived from the older software, and the discrepancy

Table 2. Bland–Altman Analysis and Paired *t*-Tests Showing the Agreement in OCT Retinal Thickness Derived from Phase 6.5 and Phase 7.0

			Limits of Agreement			
Retinal Thickness (μm)	Mean Difference (95% CI)	SD	Lower (95% CI)	Upper (95% CI)	t_{stat}	*P*
Healthy subjects ($n = 105$)						
Foveal circle	+3.00 (+1.64, +4.36)	7.00	−10.72 (−13.06, −8.37)	+16.72 (+14.37, +19.06)	+4.39	<0.001
Parafoveal rim	+9.74 (+8.41, +11.08)	6.89	−3.76 (−6.07, −1.45)	+23.25 (+20.94, +25.56)	+14.49	<0.001
Superior-hemi	+10.04 (+8.62, +11.45)	7.31	−4.28 (−6.74, −1.83)	+24.36 (+21.91, +26.81)	+14.08	<0.001
Inferior-hemi	+9.50 (+8.18, +10.81)	6.81	−3.87 (−6.13, −1.56)	+22.84 (+20.55, +25.12)	+14.29	<0.001
Tempo	+9.71 (+8.27, +11.16)	7.45	−4.88 (−7.38, −2.38)	+24.31 (+21.81, +26.81)	+13.37	<0.001
Superior	+10.02 (+8.56, +11.48)	7.56	−4.80 (−7.33, −2.26)	+24.84 (+22.30, +27.37)	+13.58	<0.001
Nasal	+9.90 (+8.44, +11.37)	7.56	−4.91 (−7.45, −2.38)	+24.72 (+22.19, +27.26)	+13.42	<0.001
Inferior	+9.46 (+8.12, +10.79)	6.90	−4.07 (−6.38, −1.75)	+22.98 (+20.67, +25.30)	+14.04	<0.001
Retinal disease ($n = 72$)						
Foveal circle	+3.65 (+1.93, +5.37)	7.33	−10.71 (−13.69, −7.74)	+18.02 (+15.04, +21.00)	+4.23	<0.001
Parafoveal rim	+6.40 (+5.33, +7.47)	4.56	−2.54 (−4.40, −0.69)	+15.35 (+13.50, +17.20)	+11.90	<0.001
Superior-hemi	+6.69 (+5.40, +7.99)	5.52	−4.13 (−6.37, −1.89)	+17.52 (+15.28, +19.76)	+10.29	<0.001
Inferior-hemi	+6.19 (+4.94, +7.45)	5.34	−4.28 (−6.45, −2.11)	+16.67 (+14.50, +18.84)	+9.84	<0.001
Tempo	+6.64 (+5.27, +8.01)	5.85	−4.82 (−7.20, −2.45)	+18.10 (+15.73, +20.48)	+9.63	<0.001
Superior	+6.43 (+4.93, +7.93)	6.38	−6.08 (−8.67, −3.49)	+18.94 (+16.35, +21.53)	+8.55	<0.001
Nasal	+6.57 (+5.06, +8.08)	6.43	−6.04 (−8.66, −3.43)	+19.18 (+16.57, +21.79)	+8.66	<0.001
Inferior	+5.96 (+4.58, +7.34)	5.89	−5.58 (−7.97, −3.19)	+17.50 (+15.11, +19.89)	+8.59	<0.001

Table 3. Bland–Altman Analysis and Paired *t*-Tests Showing the Agreement Between SRVD (Phase 6.5) and SVCD (Phase 7.0)

			Limits of Agreement			
SVCD – SRVD(% pixels)	Mean Difference (95% CI)	SD	Lower (95% CI)	Upper (95% CI)	t_{stat}	*P*
Healthy subjects ($n = 105$)						
Whole retina	–4.34 (–4.62, –4.06)	1.45	–7.19 (–7.68, –6.70)	–1.50 (–1.98, –1.01)	–30.64	<0.001
Foveal circle	–6.60 (–7.01, –6.19)	2.12	–10.74 (–11.45, –10.03)	–2.45 (–3.16, –1.74)	–31.95	<0.001
Parafoveal rim	–4.11 (–4.39, –3.82)	1.47	–7.00 (–7.49, –6.50)	–1.22 (–1.71, –0.73)	–28.57	<0.001
Superior-hemi	–4.05 (–4.36, –3.75)	1.57	–7.14 (–7.66, –6.61)	–0.97 (–1.50, –0.44)	–26.40	<0.001
Inferior-hemi	–4.17 (–4.47, –3.87)	1.54	–7.19 (–7.71, –6.67)	–1.15 (–1.67, –0.64)	–27.76	<0.001
Tempo	–4.36 (–4.69, –4.02)	1.74	–7.77 (–8.35, –7.18)	–0.95 (–1.53, –0.36)	–25.67	<0.001
Superior	–3.89 (–4.20, –3.59)	1.58	–7.00 (–7.53, –6.47)	–0.79 (–1.32, –0.26)	–25.20	<0.001
Nasal	–4.29 (–4.62, –3.97)	1.68	–7.59 (–8.15, –7.03)	–0.99 (–1.56, –0.43)	–26.14	<0.001
Inferior	–4.02 (–4.33, –3.70)	1.64	–7.23 (–7.78, –6.68)	–0.80 (–1.35, –0.25)	–25.07	<0.001
Retinal disease ($n = 72$)						
Whole retina	–4.99 (–5.49, –4.49)	2.15	–9.20 (–10.08, –8.33)	–0.78 (–1.65, +0.09)	–19.70	<0.001
Foveal circle	–7.65 (–8.51, –6.78)	3.68	–14.85 (–16.35, –13.36)	–0.44 (–1.93, +1.06)	–17.64	<0.001
Parafoveal rim	–4.68 (–5.19, –4.18)	2.15	–8.90 (–9.78, –8.03)	–0.46 (–1.34, +0.41)	–18.45	<0.001
Superior-hemi	–4.87 (–5.44, –4.30)	2.43	–9.63 (–10.62, –8.64)	–0.10 (–1.09, +0.89)	–16.99	<0.001
Inferior-hemi	–4.51 (–5.11, –3.91)	2.55	–9.51 (–10.54, –8.47)	+0.48 (–0.55, +1.52)	–15.03	<0.001
Tempo	–4.96 (–5.60, –4.33)	2.71	–10.27 (–11.37, –9.17)	+0.35 (–0.75, +1.45)	–15.55	<0.001
Superior	–4.73 (–5.43, –4.03)	2.97	–10.55 (–11.76, –9.35)	+1.09 (–0.11, +2.30)	–13.51	<0.001
Nasal	–4.45 (–4.97, –3.93)	2.22	–8.81 (–9.71, –7.91)	–0.10 (–1.00, +0.80)	–17.00	<0.001
Inferior	–4.59 (–5.23, –3.95)	2.72	–9.93 (–11.03, –8.82)	+0.75 (–0.36, +1.85)	–14.30	<0.001

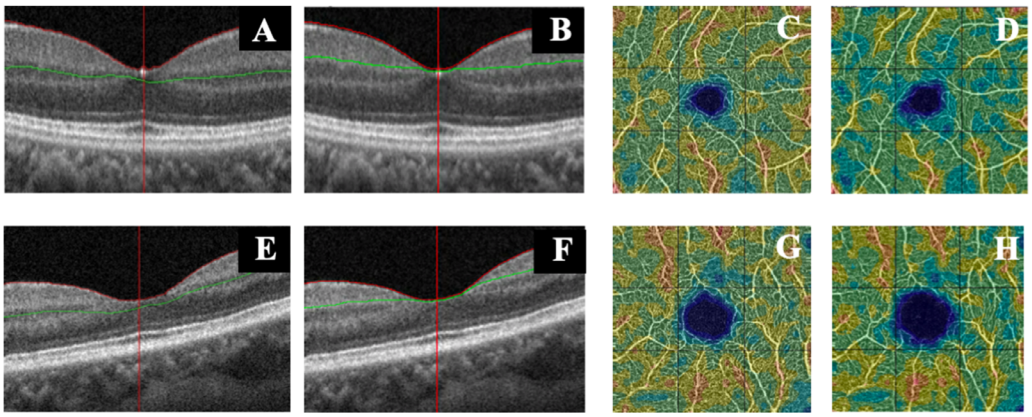

Figure 3. Illustration of the segmentation line (A, B, E, F) and density map (C, D, G, H) generated before and after the upgrade to Phase 7.0 software for healthy retina. In case 1 (A–D), the relative changes in foveal inner retinal VD and RT are –16.02% and +8%, respectively. In case 2 (E, H), the relative changes in foveal VD and RT are –44.42% and +0.92%, respectively.

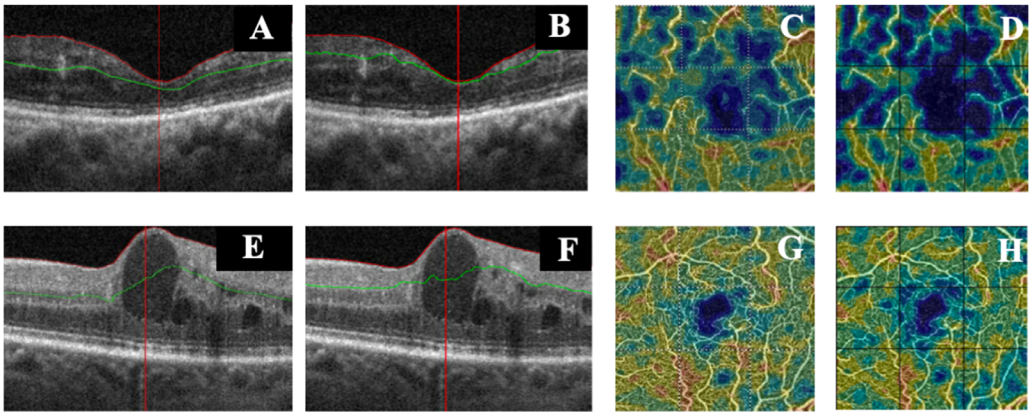

Figure 4. Illustration of the segmentation line (A, B, E, F) and density map (C, D, G, H) generated before and after the upgrade to Phase 7.0 software for diseased retina. In case 1 (A–D), a patient with diabetic retinopathy, the relative changes in foveal VD and RT are –62.14% and +0.53%; respectively. In case 2 (E–H), a patient with diabetic retinopathy, the relative changes in foveal VD and RT are +4.2% and –15.80%, respectively.

appeared to be greater for diseased eyes but not dependent on image quality. Although the difference between SRVD (Phase 6.5) and SVCD (Phase 7.0) can be readily explained by the thinner slab and removal of flow projection artifacts[21] applied in a new version of the software, it is not clear why variations are also observed in RT measurement.

The impact of different segmentation algorithm on RT measurement has been demonstrated previously when different devices were compared. Bentaleb-Machkour et al.[22] compared central macular thickness measurements obtained using the Stratus OCT (Carl Zeiss Meditec, Inc., Dublin, CA, USA), Cirrus HD-OCT (Carl Zeiss Meditec), and 3D-OCT 1000 (Topcon Corporation, Tokyo, Japan). They concluded in their study that the different OCT devices cannot be used interchangeably due to differences in the segmentation algorithms. Lammer et al.[23] compared RT measurements by four spectral OCT devices—Spectralis HRA+OCT (Heidelberg Engineering, Heidelberg, Germany), Cirrus HD-OCT, Topcon 3D OCT-1000, and Stratus OCT—and also reported a lack of inter-device agreement that seemed to be related to differences in the segmentation algorithms. The same observations have been reported by Pierro et al.,[24] who compared the measurement of retinal NFL thickness by six different devices, including Optovue OCT devices; by Sull et al.,[25] who compared RT measurements by four OCT instruments (including Optovue); and Wolf-Schmurrbusch et al.,[26] who compared central RT measurement by six OCT devices (including Optovue).

Only one report has demonstrated the impact of software upgrades in retinal segmentation algorithms on output parameters. In 2015, Hollo et al.[27] investigated the impact of a software upgrade for the Optovue

RTVue-100 OCT (version 6.3 to 6.12) for the detection of glaucoma using inner macular retinal thickness and retinal NFL thickness progression. The aim of the study was to evaluate the potential clinical usefulness of the new software version for detection of glaucomatous progression. In this study, 109 participants were investigated at 6-month intervals (mean follow-up 5 years). The authors demonstrated that measurement variability was significantly lower with the newer software version for all measured parameters and attributed the improvement to better image segmentation algorithms. To explain our observation of the unexpected increase in parafoveal RT in healthy and diseased eyes, close inspection of the segmentation lines scan by scan, before and after the software upgrade, is essential. However, the software upgrade was irreversible, and it is not possible to revert back to the older version to examine this difference. Therefore, caution is required when comparing data derived from different versions of the software on the same device. For healthy eyes, previously published RTs need to be increased by the conversion factors summarized in Table 2 before they can be compared to RTs derived from the new software version.

OCTA-derived vessel density measure can also vary significantly among devices. Munk et al.[28] compared four OCTA devices: Topcon DRI OCT Triton, Optovue RTVue XR, a prototype Spectralis OCT2, and Cirrus 5000-HD-OCT. Although they reported no significant differences in mean vessel densities among these modules, they observed a weak correlation among the devices, which suggests that artifacts and differences in slab boundary segmentation may have a significant impact on the measurement of vessel density. Lei et al.[29] tested the repeatability and reproducibility of measurements of peripapillary capillaries in the same study subjects using the Spectralis OCT2 OCTA module, RTVue XR Avanti AngioVue, Topcon DRI OCT Triton, and Cirrus HD-5000 AngioPlex OCTA instruments. Although the study revealed that the repeatability of measuring peripapillary capillaries was high for all four devices, the reproducibility among the machines was not. This was attributed to differences in the segmentation boundaries between the instruments. The same observation, that differences in segmentation algorithms and resultant boundaries preclude meaningful comparisons among OCTA devices, was also made by the Corvi et al.,[30] who compared results obtained from seven different OCT instruments. Given that the outer boundaries or superficial retinal vessels in the older Phase 6.5 software are shifted from the INL to the IPL to define the outer boundary of the superficial vascular complex in the newer Phase 7.0 version, it is not surprising that there is an overall reduction in density measures. However, it is important to note that the greater SD of the bias and LA in diseased retina suggests that segmentation errors in the altered outer boundary may reduce the accuracy of a conversion factor. For healthy eyes, previously published SRVD values may have to be reduced by the conversion factors as summarized in Table 3 prior to comparison with SVCD values derived from the new software version.

Although we were able to provide an estimate of the magnitude of the change in RT and VD from this software upgrade, there are a number of significant limitations in this study. First, the sample size was small, with the majority being affected by retinal vascular diseases (diabetic retinopathy, retinal vein occlusion, and Coats disease). The differences in thickness and density measures between the two software versions may be greater if we had access to images that showed vitreomacular traction disorders or outer retinal abnormalities. Second, we only examined the differences in the inner retinal vessels (SRV vs. SVC) in a 3 × 3-mm scanning protocol. Neither foveal avascular zone areas nor deep capillary or vascular complex densities were compared, as we did not have access to the old foveal avascular zone area calculations and there was no output for the deep retinal vessel density from the old software. We also did not export the 6 × 6-mm data prior to the upgrade. Third, we did not investigate the effect of new segmentation in the Phase 7.0 version on the test–retest variability thresholds in SVCD, as this would require a prospective study design. Fourth, although we suspected segmentation error in the ILM and Bruch's membrane as the cause of differences in RT between the two software versions, we were unable to examine every B-scan to look for segmentation error as this information could not be exported prior to upgrade. Further analysis is required to confirm the accuracy of the new segmentation algorithm compared to the previous software. Finally, we did not take into consideration the effect of image magnification due to deviation from the default axial length used by the Optovue device.

Conclusions

We demonstrated the impact of the altered segmentation algorithm and boundaries on RT and VD measurements. The unexpected change in RT measurement should be considered by users of the RTVue XR Avanti SD-OCT device when comparing outcomes of analyses before and after the software upgrade. We recommend that previously published normative

databases of retinal layer thickness and retinal vascular density, and their test–retest variability thresholds, should be recalculated using the new software for future reference.

Acknowledgments

The authors thank Natasha Vallis and Sukanya Arunachalam for their assistance with data extraction.

This work was supported by the Australian National Health and Medical Research Council Career Development Fellowship (MRF1142962, FKC) and the Centre of Research Excellence Grant (GNT1116360, FKC), and the Egyptian Ministry of Higher Education (NA)

Danuta M. Sampson and Noha Ali contributed equally to conceptualization, data extraction, data analysis, writing and proofreading of the final manuscript.

Disclosure: **D.M. Sampson**, None; **N. Ali**, None; **A.A. Yong**, None; **R. Jeewa**, None; **S. Rajgopal**, None; **D.D.C.S. Dutt**, None; **S. Mohamed**, None; **S. Mohamed**, None; **A. Hansen**, None; **M. Menghini**, None; **F.K. Chen**, None

References

1. Adhi M, Duker JS. Optical coherence tomography–current and future applications. *Curr Opin Ophthalmol*. 2013;24:213–221.
2. Bressler SB, Edwards AR, Andreoli CM, et al. Reproducibility of Optovue RTVue optical coherence tomography retinal thickness measurements and conversion to equivalent Zeiss Stratus metrics in diabetic macular edema. *Trans Vis Sci Technol*. 2015;4:1–11.
3. Danesh-Meyer HV, Papchenko T, Savino PJ, Law A, Evans J, Gamble GD. In vivo retinal nerve fiber layer thickness measured by optical coherence tomography predicts visual recovery after surgery for parachiasmal tumors. *Invest Ophthalmol Vis Sci*. 2008;49:1879–1885.
4. Drexler W, Sattmann H, Hermann B, et al. Enhanced visualization of macular pathology with the use of ultrahigh-resolution optical coherence tomography. *Arch Ophthalmol*. 2003;121:695–706.
5. Sambhav K, Grover S, Chalam KV. The application of optical coherence tomography angiography in retinal diseases. *Surv Ophthalmol*. 2017;62:838–866.
6. Iida Y, Muraoka Y, Ooto S, et al. Morphologic and functional retinal vessel changes in branch retinal vein occlusion: An optical coherence tomography angiography study. *Am J Ophthalmol*. 2017;182:168–179.
7. Agemy SA, Scripsema NK, Shah CM, et al. Retinal vascular perfusion density mapping using optical coherence tomography angiography in normals and diabetic retinopathy patients. *Retina*. 2015;35:2353–2363.
8. Yu J, Jiang C, Wang X, et al. Macular perfusion in healthy Chinese: an optical coherence tomography angiogram study macular perfusion in healthy Chinese by Angio-OCT. *Invest Ophthalmol Vis Sci*. 2015;56:3212–3217.
9. Jia Y, Tan O, Tokayer J, et al. Split-spectrum amplitude-decorrelation angiography with optical coherence tomography. *Opt Express*. 2012;20:4710–4725.
10. Coscas F, Sellam A, Glacet-Bernard A, et al. Normative data for vascular density in superficial and deep capillary plexuses of healthy adults assessed by optical coherence tomography angiography normative data for vascular density. *Invest Ophthalmol Vis Sci*. 2016;57:211–223.
11. Shahlaee A, Pefkianaki M, Hsu J, Ho AC. Measurement of foveal avascular zone dimensions and its reliability in healthy eyes using optical coherence tomography angiography. *Am J Ophthalmol*. 2016;161:50–55.
12. Hwang TS, Gao SS, Liu L, et al. Automated quantification of capillary nonperfusion using optical coherence tomography angiography in diabetic retinopathy. *JAMA Ophthalmol*. 2016;134:367–373.
13. You Q, Freeman WR, Weinreb RN, et al. Reproducibility of vessel density measurement with optical coherence tomography angiography in eyes with and without retinopathy. *Retina*. 2017;37:1475–1482.
14. Garas A, Tóth M, Vargha P, Holló G. Comparison of repeatability of retinal nerve fiber layer thickness measurement made using the RTVue Fourier-domain optical coherence tomograph and the GDx scanning laser polarimeter with variable or enhanced corneal compensation. *J Glaucoma*. 2010;19:412–417.
15. Garas A, Vargha P, Holló G. Reproducibility of retinal nerve fiber layer and macular thickness measurement with the RTVue-100 optical coherence tomograph. *Ophthalmology*. 2010;117:738–746.
16. González-García AO, Vizzeri G, Bowd C, Medeiros FA, Zangwill LM, Weinreb RN.

Reproducibility of RTVue retinal nerve fiber layer thickness and optic disc measurements and agreement with Stratus optical coherence tomography measurements. *Am J Ophthalmol*. 2009;147:1067–1074.e1.
17. Campbell JP, Zhang M, Hwang TS, et al. Detailed vascular anatomy of the human retina by projection-resolved optical coherence tomography angiography. *Sci Rep*. 2017;7:42201.
18. Lavia C, Bonnin S, Maule M, Erginay A, Tadayoni R, Gaudric A. Vessel density of superficial, intermediate, and deep capillary plexuses using optical coherence tomography angiography. *Retina*. 2019;39:247–258.
19. Scanlon PH. The English national screening programme for sight-threatening diabetic retinopathy. *J Med Screen*. 2008;15:1–4.
20. Martin Bland J, Altman D. Statistical methods for assessing agreement between two methods of clinical measurement. *Lancet*. 1986;327:307–310.
21. Zhang M, Hwang TS, Campbell JP, et al. Projection-resolved optical coherence tomographic angiography. *Biomed Opt Express*. 2016; 7:816–828.
22. Bentaleb-Machkour Z, Jouffroy E, Rabilloud M, Grange J-D, Kodjikian L. Comparison of central macular thickness measured by three OCT models and study of interoperator variability. *Sci World J*. 2012;2012:842795.
23. Lammer J, Scholda C, Prünte C, Benesch T, Schmidt-Erfurth U, Bolz M. Retinal thickness and volume measurements in diabetic macular edema: a comparison of four optical coherence tomography systems. *Retina*. 2011;31:48–55.
24. Pierro L, Gagliardi M, Iuliano L, Ambrosi A, Bandello F. Retinal nerve fiber layer thickness reproducibility using seven different OCT instruments RNFL thickness assessment by OCT instrument model. *Invest Ophthalmol Vis Sci*. 2012;53:5912–5920.
25. Sull AC, Vuong LN, Price LL, et al. Comparison of spectral/Fourier domain optical coherence tomography instruments for assessment of normal macular thickness. *Retina*. 2010;30:235–245.
26. Wolf-Schnurrbusch UEK, Ceklic L, Brinkmann CK, et al. Macular thickness measurements in healthy eyes using six different optical coherence tomography instruments. *Invest Ophthalmol Vis Sci*. 2009;50:3432–3437.
27. Holló G, Naghizadeh F. Influence of a new software version of the RTVue-100 optical coherence tomograph on the detection of glaucomatous structural progression. *Eur J Ophthalmol*. 2015;25:410–415.
28. Munk MR, Giannakaki-Zimmermann H, Berger L, et al. OCT-angiography: a qualitative and quantitative comparison of 4 OCT-A devices. *PloS One*. 2017;12:e0177059.
29. Lei J, Pei C, Wen C, Abdelfattah NS. Repeatability and reproducibility of quantification of superficial peri-papillary capillaries by four different optical coherence tomography angiography devices. *Sci Rep*. 2018;8:17866.
30. Corvi F, Pellegrini M, Erba S, Cozzi M, Staurenghi G, Giani A. Reproducibility of vessel density, fractal dimension, and foveal avascular zone using 7 different optical coherence tomography angiography devices. *Am J Ophthalmol*. 2018;186:25–31.